Ultrasonic needle tracking with dynamic electronic focusing

Sunish J. Mathews[1,2,*], Dzhoshkun I. Shakir[2,3], Charles A. Mosse[1,2], Wenfeng Xia[3], Edward Z. Zhang[1,2], Paul C. Beard[1,2], Simeon J. West[1,4] Anna L. David[1,5], Sebastien Ourselin[3], Tom Vercauteren[3] and Adrien E. Desjardins[1,2]

[1] Wellcome/EPSRC Centre for Interventional and Surgical Sciences, London, UK

[2] Department of Medical Physics and Biomedical Engineering, University College London, UK

[3] School of Biomedical Engineering and Imaging Sciences, King's College London, London, UK

[4] Department of Anaesthesia, University College Hospital, London, UK

[5] Institute for Women's Health, University College London, London, UK

*Corresponding author email: sunish.mathews@ucl.ac.uk

*Phone: +44 7821730178

Abstract:

Accurate identification of the needle tip is a key challenge with ultrasound-guided percutaneous interventions in regional anaesthesia, foetal surgery and cardiovascular medicine. In this study, we developed an ultrasonic needle tracking system in which the measured needle tip location was used to set the electronic focus of the external ultrasound imaging probe. In this system, needle tip tracking was enabled with a fibre optic ultrasound sensor that was integrated into a needle stylet, and the A-lines recorded by the sensor were processed to generate tracking images of the needle tip. The needle tip position was estimated from the tracking images. The dependency of the tracking image on the electronic focal depth of the external ultrasound imaging probe was studied in a water bath and with needle insertions into a clinical training phantom. The variability in the estimated tracked position of the needle tip, with the needle tip at fixed depths in the imaging plane across a depth range from 0.5 cm – 7.5 cm, was studied. When the electronic focus was fixed, the variability of tracked position was found to increase with distance from that focus. The variability with the fixed focus was found to depend on the the relative distance between the needle tip and focal depth. It is demonstrated that with dynamic focusing, the maximum variability of tracked position was below 0.31 mm, as compared with 3.97 mm for a fixed focus.

Keywords: Ultrasound guided needle intervention, ultrasonic needle tracking, needle tip localization, fiber optic ultrasound sensor, Fabry-Perot interferometer, interventional ultrasound

Introduction

Ultrasound (US) image guidance is routinely used in clinical practice to guide needle-based percutaneous procedures such as for the delivery of regional anaesthesia, tumour biopsies, central venous access in cardiology and foetal medicine (Chin et al. 2008, Holm and Skjoldbye 1986, Khati et al. 2011, Leibowitz et al. 2020, Morris and Weston 1998). A key challenge associated with ultrasound-guided needle insertions is the efficient and accurate identification of the needle tip. In-plane approaches require good hand-eye coordination to keep the needle in the imaging plane as it is advanced to the target. These challenges are particularly acute when the needle tip is at high depths (> 5 cm), when the insertion angle is steep and when the needle diameter is small (e.g., 22G or higher) so that out-of-plane deflection takes place during insertions (Brambati et al. 1987, Ghi et al. 2016). Even for experienced clinicians, the needle can readily stray from the imaging plane and damage a critical structure (Smith et al. 1998).

Various techniques have been proposed to improve the visibility of the needle tip in ultrasound-guided needle interventions (Beigi et al. 2021, McLeod 2021, Van de Berg et al. 2019). These include the use of echogenic needles, camera-based tracking, electromagnetic tracking, and ultrasonic needle tracking with the use of an integrated sensor, actuator or transmitter in the needle (Hebard and Graham 2011, Levy et al. 2007, Nikolov and Jorgen 2008, Najafi et al. 2015, Mung et al. 2011, Guo et al. 2014, Cheng et al. 2018, Xia et al. 2017). Ultrasonic needle tracking with the use of a fibre optic ultrasound sensor (FOUS) positioned at the needle tip has shown good promise recently and has been demonstrated for both 2D and 3D tracking (Xia et al. 2015, 2017). Previous implementations by our group used two alternating sequences of ultrasound transmissions: one with electronic focusing for US imaging and a second with transmissions by individual elements for US tracking. With the latter sequence, the A-lines recorded by the FOUS are processed to generate a tracking image, in which the only object is the needle tip. There are two main limitations of this paradigm. First, the use of two sequences results in a two-fold reduction in effective imaging rate. Second, single-element

transmissions can have high divergence in-plane relative to electronically-focused transmissions, which leads to lower hydrophone signal magnitudes in the tracking images, which could necessitate computationally expensive algorithms to improve the SNR.

An alternative paradigm for needle tracking with a FOUS, which could overcome the aforementioned limitations, involves the use of only one sequence of electronically focussed transmissions that is used for both US imaging and tracking. Within this paradigm, if there is a fixed electronic focus, a primary challenge that arises is that the lateral width of the needle tip in the tracking image is highly dependent on the axial distance of the needle tip relative to that focus. It was previously been demonstrated that as these widths increase, there is a corresponding decrease in the accuracy with which the needle tip locations can be measured from the tracking images (Mari et al. 2014).

The solution we propose here is to perform US tracking with a single sequence of electronically focused transmissions, and dynamically adjust the electronic focus based on the measured axial location of the needle tip. We present a fully functional system with this capability, which includes a real-time needle tracking system based on a FOUS. The sensor is integrated within the needle using a novel withdrawable stylet design that can be tailored to suit different needle types and therefore different clinical procedures. We study the impact of the US electronic focus on the reconstructed image of the needle tip and estimate the variability in the tracked needle tip positions with fixed US focus and with focus tracking in a water bath and a clinical phantom.

Materials and Methods

Ultrasonic needle tracking system overview

The US needle tracking (UNT) system was designed at the outset to be compatible with clinical B-mode imaging. A schematic overview is shown in Figure 1. The system uses a clinical US imaging

system (Ultrasonix MPD, BK Medical, UK) with a linear array imaging probe (L14-5/38, 128 elements, linear array transducer, 14-5 MHz) for 2D imaging. A primary element of the tracking system is a custom-designed console as shown in Figure 1(a). The ultrasonic needle tracking system comprises the medical device which is a needle with an integrated FOUS (Figure 1 (b)). The FOUS receives the electronically focussed transmissions from the imaging probe, which are processed on the tracking console to estimate the needle tip positions. When the needle tip is away from the US focus, the FOUS receives a diverging US scan-line and receives the signal from several scan-lines adjacent to the direct line-of-sight position. This results in the needle tip image having an extended span in the lateral direction. On the other hand, when the needle tip is at the same depth as the US focus, the FOUS receives the signal from only a few scan-lines that are directly in the line-of-sight and is likely to have a localized needle tip image (Figure 1 (c)).

The system also captures the live B-mode US images from the US imaging system. The tracked positions of the needle tip are then overlaid on the live US images on the monitor on the tracking console system, where the user can see the US images together with the active position of the needle tip.

Ultrasound Receiver: Fibre Optic Ultrasound Sensor

Reception of the ultrasound transmissions from the imaging probe within the needle was performed by a high finesse Fabry-Pérot (F-P) cavity interferometer-based FOUS. The FOUS was custom-built using methods previously described (Zhang and Beard 2011, Guggenheim et al. 2017). Briefly, the ultrasound sensing element was fabricated on the tip of the fibre, with thin film reflective coatings and a polymer spacer to form a plano-concave F-P cavity. The optical thickness of the F-P cavity is modulated by impinging ultrasound waves, and detected as a change of the intensity of reflected interrogation light. The FOUS, is particularly suited for needle tracking as it has been demonstrated to have an omnidirectional frequency response (Zhang and Beard 2015) so that it is

117 independent of the needle insertion angle. The sensor used for the studies had a measured noise
118 equivalent pressure of ~ 350 Pa in a detection bandwidth of 20 MHz and a good frequency-dependent
119 directivity response for incidence angles ranging from -165° to 165° (Mathews et al. 2019).

120 *Needle with Integrated Fibre Optic Ultrasound Sensor*

121 In this study, we chose a commercial, 22G spinal needle (OD: 0.71 mm) (BD Medical, USA) with a
122 length of 90 mm that is widely used in percutaneous interventions across different clinical application
123 spaces. The FOUS was integrated inside a custom-built stylet to fit inside the cannula of the
124 commercial needle. The stylet was fabricated using a 27G (OD: 0.41 mm) hypodermic tube and was
125 designed to match the dimension of the stylet which is provided with the commercial needle. A
126 microscope image of the needle tip with the stylet and the integrated FOUS is shown in Figure 1 (b).

127

128 *Needle tracking console: data acquisition*

129 For real-time ultrasound needle tracking, we developed a tracking console that connects to the
130 needle with a FOUS and receives the US transmission from the imaging probe of the US system. The
131 tracking console registers the trigger signals from the US imaging system and uses these to process
132 the FOUS signals to form an image of the needle tip, which is used to estimate the needle tip
133 coordinates in the imaging plane of the US probe. A system-level block diagram of the real-time needle
134 tracking console is shown in Figure 2. The interrogation of the FOUS was done by an external cavity
135 wavelength-tunable laser (Santec TSL-550, Santec Europe Ltd, UK) with a tuning range from 1500–
136 1630 nm. The laser was coupled into the FOUS using a fibre optic circulator and the reflected light
137 from the F-P cavity sensing element of the sensor was directed onto a photo-receiver system.

138 The photo-receiver system comprises an InGaAs photodiode-transimpedance amplifier unit that
139 generates low (V_{lf}) and high frequency (V_{hf}) output voltage signals. These were acquired in the needle
140 tracking workstation, where the V_{lf} was acquired using a multifunction I/O device (PCIe-6323, National

Instruments, UK), which was digitized at 16 bits with a sampling rate of 250 kS/s. The received ultrasound signal, V_{hf}, was acquired using a high-speed digitizer (PCI-5114, 125 MHz Bandwidth, National Instruments, UK), and was digitized at 8 bits at a sampling rate of 250 MS/s. The FOUS interrogation software uses the low-frequency signal to measure the transfer function of the F-P cavity and determine the interrogation wavelength of the tunable laser (via GPIB control) that provides the maximum sensitivity (Zhang et al. 2008).

The high-speed digitizer uses the trigger outputs from the US imaging system (grey blocks on the top). The acquisition of the digitizer was triggered by the output frame trigger which is the start of each B-mode US frame. The digitizer then synchronously acquired both the line trigger (start of individual A-lines) from the US system and the high-frequency FOUS signal from the photo-receiver. These FOUS signals were processed through a parsing algorithm that applies a band-pass filter and computes the signal envelope using a Hilbert Transform. The parsing was based on the reception of the line triggers and the estimated relative delays in receiving the US signals from the elements of the US imaging probe by the FOUS. The algorithm converts the 1-D FOUS signal (a series of A-lines in one imaging frame) to a 2-D reconstructed image of the needle tip. This was done by a custom-built tracking application software developed in LabVIEW. The position of the needle tip was estimated in the coordinate system of the US imaging probe for overlay and passed on to the graphical user interface (GUI) of the application software. The rate of the overlay on the tracking system was approximately 10 Hz.

Needle tracking console: image capture and dynamic focusing

The console acquires the live stream of US images from the US imaging system through an Ethernet port on the tracking workstation. The acquisition of the US images was enabled using a custom LabVIEW compatible extensible C++ application programming interface (API) (Shakir and Mathews 2019), that is interfaced with the commercial software development kit (SDK) of the Ultrasonix MDP

imaging system (Figure 2; grey blocks on top). The API allows for real-time capture of the US frames at an acquisition rate of over 60 frames per second. The US frames acquired as 1-D low-level metadata was passed on to the tracking software, which converts it into 2-D B-mode US images based on the image size set on the US imaging system. The US images were then passed on to the GUI as shown in Figure 2.

In addition to real-time frame capture, the API can control the imaging parameters on the US imaging system provided by the SDK. This allows the API to set the focal depth of the probe through the tracking application software. The real-time focus tracking was achieved by the software by first estimating the depth of the needle tip using the signals acquired by the high-speed digitizer and then using the estimated depth of the needle to dynamically reset the focal depth of the US imaging probe to the depth of the needle tip.

Impact of US focus and needle tip variability

To study the impact of the position of the US electronic focus on the needle tip image, the needle was inserted into a clinical training phantom (Adam, Rouilly Ltd, UK) and needle tip images were acquired at various focal depths. The depth of the needle tip was fixed at ~ 4.02 cm and the US focal depth was varied from 0.5 cm – 7.5 cm. For each focal depth, the needle tip images were recorded by the acquisition system and post-processed in MATLAB. This post-processing comprised maximum intensity projections (MIPs) along the lateral (scan axis) and axial (depth axis) directions. Gaussian fitting was applied to the MIPs in each direction; the full width at half maximum (FWHM) was calculated from those fits and used as measures of the lateral and axial spread of the needle tip image. The SNR was estimated from needle tip images by taking the ratio of the maximum amplitude of the FOUS signal and the estimated standard deviation of the noise floor from an empirically chosen region of the 2-D needle tip image.

The needle tip positions were estimated based on both the coordinates of the maxima of the reconstructed needle tip image and also on the centre of mass (CoM) of a region of interest (ROI) around the position of the maxima. To estimate the CoM, a region of interest with 100 × 120 pixels was selected from the needle tip image based on the position of the maximum. Prior to the calculation of CoM, background subtraction was applied and then thresholding was applied to the ROI such that coordinates with less than ~ 70% of the maximum intensity are zeroed, to obtain an accurate representation of the shape of the needle tip image. The CoM was then estimated based on the average of all positions weighted by the intensity at each position in the ROI.

The impact of a fixed focus on the variability of the needle tip position along the axial and lateral directions in the imaging plane was studied. To measure the variability, the needle with a FOUS was positioned inside a water tank directly under the US probe in the imaging plane. The needle tip images were recorded sequentially for over 100 US frames, with the needle tip fixed inside a water bath. The variability in the needle tip coordinate (for both axial and lateral) is defined as the absolute value of the difference between the mean of the coordinate over the 100 US frames and the estimated coordinate for each frame. The maximum value of the variability along both the lateral and axial direction are taken as the maximum variability. Here we make the distinction between maximum variability and absolute accuracy of tracking. The former quantity is taken to be a relative measure that describes how the needle tip position estimates from the UNT change across frames; the latter, which is not measured here, relates to a ground truth position of the needle tip.

The variability estimation was performed on both the needle tip positions based on maxima and the CoM and the maximum variability in these positions were estimated with both fixed US focus and with focus tracking. For the fixed focus case, the US focal depth was fixed at 4.18 cm, and the needle was translated inside the water bath to have it positioned at various depths from ~ 1.5 cm to 6.5 cm. For the focus tracking case, the needle was translated and positioned in the same depth range.

Results

Impact of US focus on the image of the needle tip

The 2-D needle tip images acquired for a fixed position of the needle tip (~ 4.02 cm) in a focal depth range from 1.0 cm – 7.0 cm are shown in Figure 3(a). For shallower (1 cm – 3 cm) and deeper (5 cm – 7 cm) positions of focal depths relative to the depth of the needle tip, the image of the needle tip had an extended lateral span. When the focal depth (4 cm) was coincident with the needle tip, the 2-D needle tip image was a localized spot in the imaging plane.

Figure 3(b) shows the FWHM in the lateral and axial directions for the needle tip images recorded at depths ranging from 0.5 cm – 7.5 cm, in increments of 0.5 cm. The FWHM in lateral direction varies significantly with the axial position of the US focal depth. The values were highest for focal depths 0.5 cm (FWHM = 11.06 mm) and 7.5 cm (FWHM = 10.02 cm) and was estimated to be the least at a focal depth of 4 cm (FWHM = 1.02 mm), where the needle tip (fixed at 4.02 cm) is coincident with the position of the US focal depth. The FWHM in the axial direction is marginally impacted by the position of the US focal depth. The estimated values were in the range from 0.487 mm – 1.11 mm. Figure 3(b) also shows how the signal-to-noise ratio (SNR) of the 2-D needle tip image varies with the focal depth. A maximum SNR of ~ 165 was measured when the focal depth was at ~ 4.0 cm. The SNR reduces when the focal depth was set above or below the depth of the needle tip. A minimum SNR of ~ 20 (a relative drop of 88% from maximum) was measured at the focal depth of 0.5 cm.

Variability of needle tip position with US focal depth

For the case where the electronic focus was fixed (4.18 cm; Figure 4a), the needle tip images obtained far from the focus (1.73 cm and 6.61 cm) had extended lateral spans. The lateral span was considerably smaller when the needle tip was positioned at the US focus. For the case with focus tracking, a small lateral span was consistently obtained across this depth range (1.69 cm, 3.95 cm and

6.49 cm; Figure 4b). Figure 4(c) and (d) summarise the maximum variability in estimated needle tip positions (axial and lateral) based on both the maximum and CoM, with fixed US focus and with focus tracking. Along the lateral direction (Figure 4(a)), the variability of needle tip positions was the highest in the case with fixed US focus and when the maximum was used as the position of the needle tip. The highest value for maximum variability was estimated as 3.97 mm at a depth of ~ 1.73 mm and the lowest value of ~ 0.33 mm was estimated at a depth of ~ 4.17 mm. For needle tip positions based on the CoM, the variability was lower in comparison. The estimated values ranged between a maximum of 1.33 mm to a minimum of 0.22 mm. The variability was maximal when the needle was further away from the position of the focal depth on either side of the fixed US focus. The variability was the least with the focus tracking feature on as can be seen in Figure 4(a). The estimated values were found to be in the range from 0.12 mm – 0.31 mm for the depth range from 1.73 cm – 6.61 cm.

Figure 4(b) shows the variability with the needle tip position in the axial direction for all three cases (maximum, CoM for fixed focus and with focus tracking). For the coordinates based on the maximum of the needle tip image, the maximum variability was estimated to be in the range from 0.21 mm – 0.38 mm. For the CoM based needle tip positions the maximum variability in the axial direction was estimated to be in the range from 0.046 mm – 0.106 mm. With focus tracking, the maximum variability was approximately 0.05 mm across a depth range from 1.73 cm – 6.61 cm. In the axial direction, the variability did not have any dependency on the US focal depth.

Discussion

One prominent challenge for clinicians with procedures that involve deep target insertions is the fixed position of the US electronic focus of the imaging probe during the procedure. It is quite well known that the dynamic US focus feature provided by the modern US imaging system improves the resolution of the US image (Manes et al. 1988, Powers and Kremkau 2011). For deep target needle insertions, clinicians set the US focal depth based on the depth of the target and/or the envisaged

needle insertion path and is normally not changed during the procedure, particularly because of the requirement to manually reset the focus on the US system. During the needle insertion, this can lead to a poor resolution in the US image at depths above and below the set depth of the US focus. Although advanced US imaging systems can provide multiple US transmit foci, this feature results in a reduction of the frame rate (Powers and Kremkau 2011). The focus tracking feature, which has been demonstrated with the system here, can provide dynamic focusing without reduction in imaging frame rate together with real-time needle tip tracking.

The major advantage provided by the UNT system presented in this paper, is the reduction in frame-to-frame variability of the tracked positions of the needle tip. The FOUS in the needle receives the signals from the elements of the US imaging probe with relatively varied delays depending on where the electronic focus was set. For shallower and deeper focal depths relative to the depth of the needle, the 2-D reconstructed images of the needle tip were spread laterally across the US imaging plane. When the needle tip was at the US focus, the FOUS receives the signals from the elements of the US imaging probe with the least relative delays and the 2-D needle tip image was more like a localized spot in the US imaging plane as observed in figure 3(a) with the needle in the phantom. In the axial direction, the shape of the needle tip image primarily depends on the frequency response of the FOUS and is mostly found to be similar with changing depth and the position of the ultrasound focus (Figure 3(b)).

With the focusing of ultrasound to the depth of the needle tip, the FOUS receives a stronger signal due to constructive interference of US signals from the maximum number of elements of the imaging probe that are in the line-of-sight. In the case of the needle in the clinical training phantom, the SNR of the FOUS signal was highest when the US focus is set axially closer to the depth of the needle tip. The studies into the impact of US focus demonstrate that the FOUS signal will have good SNR and a spatially localized 2-D needle tip image when the needle tip coincides with the US focal depth.

The use of CoM for the estimation of needle tip coordinates reduces the randomization of the position of the maximum caused due to noise in the acquisition system. As a result, the variability in estimated needle tip positions based on CoM are consistently lower in comparison to the needle tip position based on maxima. However, with a fixed US electronic focus, the variability in the lateral direction (figure 4(a)) is highly dependent on the position of the focal depth. This is due to the prominent broadening feature of the reconstructed needle tip image in the lateral direction (figure 3(a)), caused by the variations in the delays in receiving the signals from the elements of the US imaging probe by the FOUS. With a laterally-broadened image of the needle tip, the variability of the lateral position of the maximum from frame-to-frame will increase, although the CoM based estimation helps in reducing this variability, it is still dependant on the shape of the needle tip image. With real-time focus tracking, the needle tip images are locally confined in the US imaging plane due to the focus of the ultrasound probe being reset to the depth of the needle tip. The variability estimates with the needle in the water bath show the maximum variability were the lowest (for both lateral and lateral and axial directions) with the real-time focus tracking. Lower frame-to-frame variability is useful to improve tracking accuracy. However, to estimate the tracking accuracy, a measure of the ground truth for the needle tip position is required for comparison. There are several methods for estimating this ground truth, including the use of an additional imaging modality (for instance, multi-axis fluoroscopy) or with linear translation stages, as described in Xia et al. 2017.

Several improvements to the system presented here can be envisaged. The effective frame rate (ca. 10 Hz) was limited by the digitizer used that had a single trigger input. Data acquisition level parsing of the FOUS signals can be implemented by using a digitizer card with two or more trigger inputs, which will eliminate the need to apply a parsing algorithm post signal acquisition. In future implementations, the processing and visualizing of US and tracking image data could be more efficiently handled with the use of high-speed image acquisition and tracking image processing using a graphical processing unit (GPU). In this way, the effective frame rate could be improved substantially to match the frame rate of the US imaging system (25 Hz - 30 Hz).

Conclusions

In conclusion, we have demonstrated for the first time a fibre optic ultrasound sensor based real-time US needle tracking system with dynamic electronic focusing. With US focus tracking, the electronic focus of the US imaging probe can be set based on the estimated needle depth, which allows for dynamic focusing based on the point of interest of the medical device. The SNR is shown to improve with focus tracking and the variability in estimating the needle tip position along the lateral direction is shown to have reduced with the maximum variability estimated to be below 0.31 mm. Both these factors will reduce the uncertainty in estimating the absolute needle tip positions and improve the absolute accuracy of needle tracking with FOUS integrated needles in ultrasonic needle tracking systems.

Focus tracking ensures dynamic focusing can be achieved without a reduction in the imaging frame rate, which could avoid the need to set a fixed focus or multiple US foci prior to the start of the clinical procedure, and also avoid the need to reset or change the focal depth during the procedure. Dynamic focus tracking also ensures that the transmit focus of the US probe is near the physical depth of the needle tip, which would provide the best possible US image quality for the anatomy near the needle tip and in the region of interest. The real-time focus tracking feature of the system is attractive in the space of foetal medicines with longer needles (≥ 8 cm) for deep target insertions, for procedures such as amniocentesis, chorionic villus sampling and foetal heart surgery.

Acknowledgements

The authors would like to acknowledge the feedback and useful insights received from Dr. Brian Dromey, Dr. Callum Little, Dr. Malcolm Finlay and Dr. Yada Kunpalin, on the clinical applications of the system.

This work was supported by the Wellcome/EPSRC Centre for Interventional and Surgical Sciences (WEISS) (203145Z/16/Z). The work is also supported by an Innovative Engineering for Health award by the Wellcome Trust (No. WT101957) and the Engineering and Physical Sciences Research Council (EPSRC) (No. NS/A000027/1). The work is also supported by a Starting Grant from the European Research Council (Grant No. ERC-2012-StG, Proposal 310970 MOPHIM), and by an EPSRC First Grant (No. EP/J010952/1). This work was also supported by ERC advance grant 74119 and by core funding from the Wellcome/EPSRC [WT203148/Z/16/Z; NS/A000049/1].

Conflict of interest statement

The authors declare that there are no conflicting interests

References

Beigi P, Salcudean SE, Ng GC, Rohling R. **Enhancement of needle visualization and localization in ultrasound.** *Int J Comp Assist Rad* 2021;16;169-178.

Brambati B, Oldrini A, Lanzani A. **Transabdominal chorionic villus sampling: a freehand ultrasound-guided technique**. *Am J Obstet Gynecol* 1978;157;134-137.

Cheng A, Zhang B, Oh P, Boctor EM. **Fusing acoustic and optical sensing for needle tracking with ultrasound.** *Proc SPIE 10576, Medical Imaging 2018: Image-Guided Procedures, Robotic Interventions, and Modelling* 2018;1057621.

Chin K, Perlas A, Chan V and Brull R. **Needle visualization in ultrasound-guided regional anaesthesia: challenges and solutions.** *Reg Anesth Pain Med* 2008;33;532-544.

Ghi T, Sotiriadis A, Calda P, Da Silva Costa F, Raine-Fenning A, Alfirevis Z and McGillivary G. **ISUOG practice guidelines: invasive procedures for prenatal diagnosis.** *Ultrasound Obstet Gynecol* 2016;48;256-268.

Guggenheim JA, Li J, Thomas TJ, Colchester RJ, Noimark S, Ogunlade O, Parkin IP, Papkonstantinou I, Desjardins AE, Zhang EZ, Beard PC. **Ultrasensitive plano-concave optical microresonators for ultrasound sensing.** *Nat Photon* 2017;11;714-719.

Guo X, Tavakoli B, Kang HJ, Kang JU, Etienne-Cummings R, Boctor EM. **Photoacoustic active ultrasound element for catheter tracking.** *Proc SPIE 8943, Photons Plus Ultrasound: Imaging and Sensing* 2014;89435M.

Hebard S, Graham H. **Echogenic technology can improve needle visibility during ultrasound-guided regional anaesthesia.** *Reg Anesth Pain Med* 2011;36;185-189.

Holm HH, Skjoldbye B. **Interventional Ultrasound.** *Ultrasound Med Bio* 1996;22;773-789.

Khati NJ, Gorodenker J, Hill MC. **Ultrasound-guided biopsies of the abdomen.** *Ultrasound Q.* 2011;27;255-268.

Leibowitz A, Oren-Grinberg A, Matyal R. **Ultrasound guidance for central venous access: current evidence and clinical recommendations.** *J Intensive Care Med.* 2020;35;303-321.

Levy EB, Tang J, Lindisch D, Glossop N, Banovac F, Cleary K. **Implementation of an electromagnetic tracking system for accurate intrahepatic puncture needle guidance: accuracy results in an in vitro model.** *Acad Radiol* 2007;14;344-354

Manes G, Tortoli P, Andreuccetti F, Avitabile G, Atzeni C. **Synchronous dynamic focusing for ultrasound imaging.** *IEEE Trans Ultrasound Ferroelectr Freq Control* 1988;20;35;14-21.

Mari JM, West SJ, Beard PC, Desjardins AE. **Needle-tip localization using an optical fibre hydrophone.** *Proc SPIE 8938, Optical Fibers and Sensors for Medical Diagnostics and Treatment Applications XIV 8938* 2014;893804.

Mathews SJ, Mosse S, Xia W, Shakir DI, Kunpalin Y, Zhang EZ, Beard PC, West SJ, David AL, Desjardins AE. **Ultrasonic needle tracking with a high-finesse Fabry-Perot fibre optic hydrophone.** *Proc SPIE 10868, Advanced Biomedical and Clinical Diagnostic and Surgical Guidance Systems XVII* 2019;108681D.

McLeod GA. **Novel approaches to needle tracking and visualization.** *Anesth* 2021;76;160-170.

Morris J, Weston MJ. **Ultrasound guided intervention in gynaecology – a review.** *BMUS Bulletin* 1998;6;26-29.

Mung J, Vignon F, Jain A. **A non-disruptive technology for robust 3D tool tracking for ultrasound-guided interventions.** *In: Fichtinger G., Martel A., Peters T. (eds) Medical Image Computing and Computer-Assisted Intervention – MICCAI 2011. Lecture Notes in Computer Science 2011;6891.*

Najafi M, Abolmaesumi P, Rohling R. **Single-camera closed-form real-time needle tracking for ultrasound-guided needle insertion.** *Ultrasound Med Bio* 2015;41;2663-2676.

Nikolov SI, Jorgen AJ. **Precision of needle tip localization using a receiver in the needle.** *IEEE Int Ultra Sym* 2008;479-482.

Powers J, Kremkau F. **Medical ultrasound systems.** *Interface Focus* 2011;1;477-489.

Shakir DI, Mathews SJ. **Xono2L,** https://github.com/gift-surg/Xono2L/ 2019.

Smith JF, Bergmann M, Gildersleeve R, Allen R. **A simple model for learning stereotactic skills in ultrasound-guided amniocentesis.** *Obstet Gynecol* 1998;92;303-305

Van de Berg NJ, Sanchez-Margallo JA, Van Dijke AP, Lango T, Van den Dobbelsteen AA. **A methodical quantification of needle visibility and echogenicity in ultrasound images.** *Ultrasound Med Bio* 2019;45;998-1009.

Xia W, Mari JM, West SJ, Ginsburg Y, David AL, Ourselin S and Desjardins AE. **In-plane ultrasonic needle tracking using a fibre-optic hydrophone.** *Med Phys* 2015;42;5983-5991.

Xia W, Noimark S, Ourselin S, West SJ, Finlay MC, David AL, Desjardins AE. **Ultrasonic Needle Tracking with a Fibre-Optic Ultrasound Transmitter for Guidance of Minimally Invasive Fetal Surgery.** *In: Descoteaux M., Maier-Hein L., Franz A., Jannin P., Collins D., Duchesne S. (eds) Medical Image Computing and Computer-Assisted Intervention − MICCAI 2017. Lecture Notes in Computer Science* 2017;10434.

Xia W, West SJ, Finlay MC, Mari JM, Ourselin S, David AL, Desjardins AE. **Looking beyond the imaging plane: 3D needle tracking with a linear array ultrasound probe.** *Sci Rep* 2017;7;3674.

Zhang EZ, Beard PC. **A miniature all-optical photoacoustic imaging probe.** *Proc SPIE 7899, Photons Plus Ultrasound: Imaging and Sensing* 2011;78991F.

413 Zhang EZ, Beard PC. **Characteristics of optimized fibre-optic ultrasound receivers for minimally**
414 **invasive photoacoustic detection.** *Proc SPIE 9323, Photon Plus Ultrasound: Imaging and Sensing*
415 2015;932311.

416 Zhang EZ, Laufer J, Beard PC. **Backward-mode multiwavelength photoacoustic scanner using a planar**
417 **Fabry-Perot polymer film ultrasound sensor for high-resolution three-dimensional imaging of**
418 **biological tissues.** *Appl Opt* 2008;47;561–577.

419

420

421

422

423

424

425

426

427

428

429

430

431

432

Figure Captions List

Figure 1:

Schematic with the overview of the ultrasonic needle tracking system.

(a) Showing the needle with fibre optic ultrasound sensor (FOUS), tracking console, ultrasound imaging system and its imaging probe, (b) Microscope image of the 22G needle tip, with the 27G stylet and the sensing element (green) at the end of the FOUS, and (c) Schematic showing the reception of electronically focused transmission from the US imaging probe, by the needle with the FOUS at the needle tip. Two scenarios are shown, first with the needle tip away from US focus (top) and second with the needle tip at US focus (bottom). The corresponding needle tip images formed by the signals received by the FOUS are shown on the right in both cases.

Figure 2:

System level block diagram of the ultrasonic needle tracking system.

The hardware components are shown on the left and the software components are shown on the right. The electronic connections are shown using black solid lines and optical connections are shown with red solid lines. The associated software communications and data flow are shown using dashed lines. Yellow blocks correspond to the needle, the FOUS console and the associated FOUS interrogation software; Blue blocks correspond to the needle tracking workstation, software and GUI; Grey blocks correspond to the US imaging probe, US imaging system and the application programming interface. The green dotted lines show focus tracking.

Figure 3:

Impact of US focus on needle tip image.

(a) 2-D needle tip images acquired with fixed US focus at depths ranging from 1.0 cm – 7.0 cm. (b) A plot showing the FWHM of the needle tip images along the axial and lateral direction, together with SNR for the FOUS signal. The US focal depth was varied from 0.5 cm – 7.5 cm. The needle tip was fixed at a depth of 4.02 cm in the imaging plane.

Figure 4:

Variability of the needle tip position with US focal depth.

(a) Needle tip images at depths 1.73 cm (a_1), 4.17 cm (a_2) and 6.61 cm (a_3), with fixed US focus at 4.18 cm, (b) Needle tip images with focus tracking at depths 1.69 cm (b_1), 3.95 cm (b_2) and 6.49 cm (b_3). The needle tip images are normalized to their individual maximum intensities. (c,d) Maximum variability for fixed focal depth (at ~ 4.18 cm) and focus tracking, estimated using the position of maximum and the centre of mass:(c) along the lateral direction (c), and along the axial direction (d). The datapoints corresponding to needle tip images (a_1), (a_2), (a_3), (b_1), (b_2), and (b_3) are indicated.

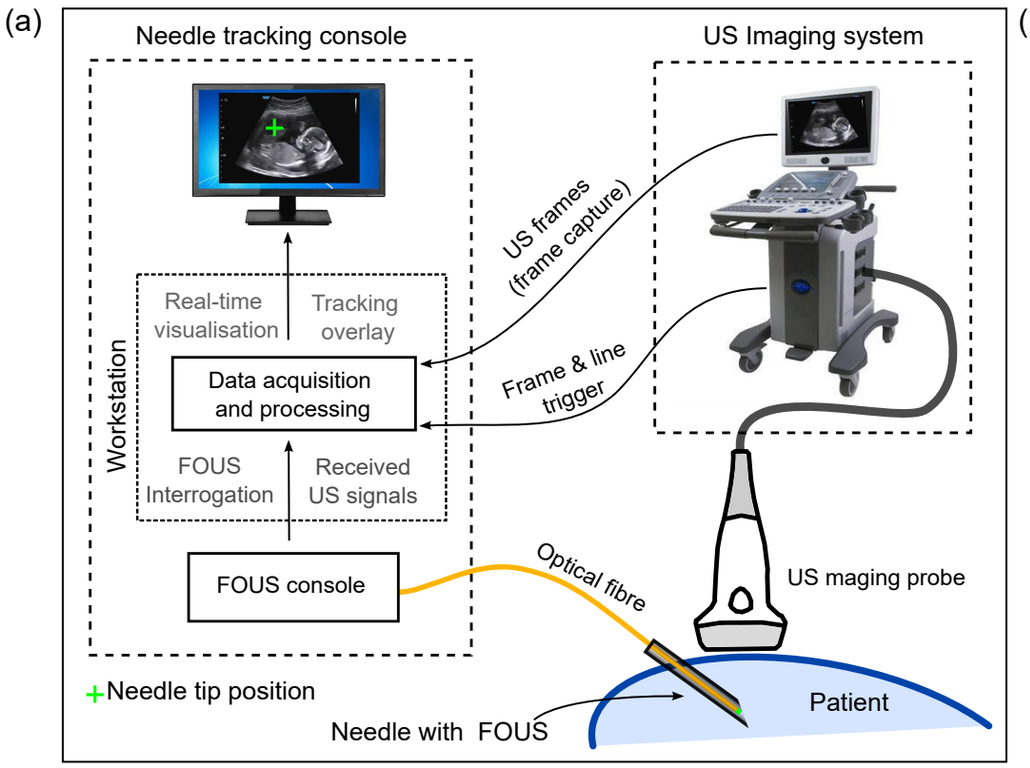
(a)
Needle tracking console
US Imaging system
Real-time visualisation
Tracking overlay
Workstation
Data acquisition and processing
FOUS Interrogation
Received US signals
FOUS console
US frames (frame capture)
Frame & line trigger
Optical fibre
US maging probe
Needle tip position
Needle with FOUS
Patient

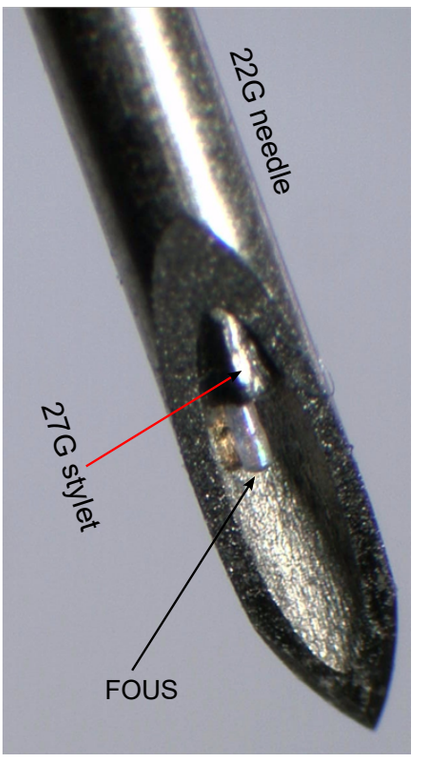
(b)
22G needle
27G stylet
FOUS

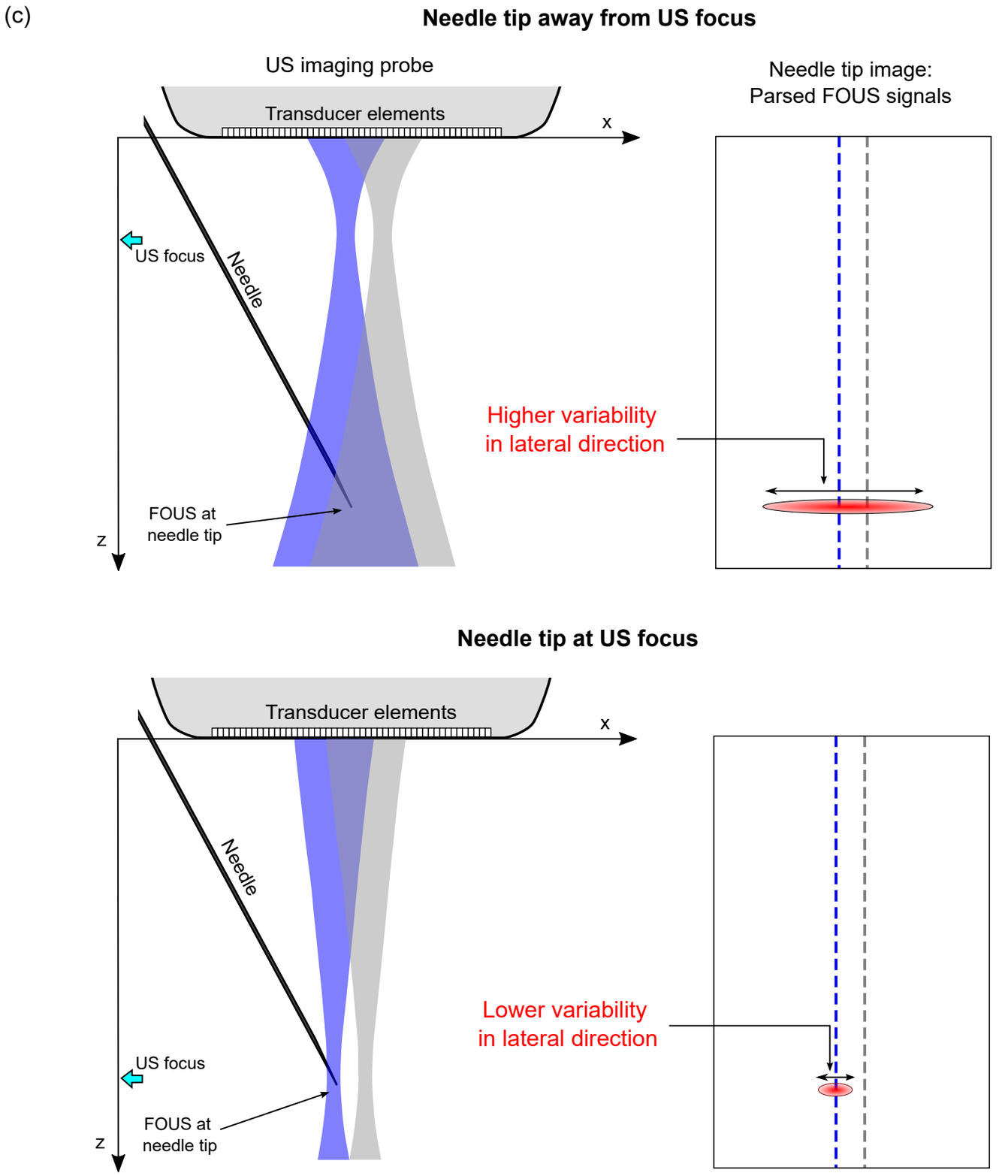
(c)
Needle tip away from US focus
US imaging probe
Transducer elements
x
US focus
Needle
FOUS at needle tip
z
Needle tip image: Parsed FOUS signals
Higher variability in lateral direction
Needle tip at US focus
Transducer elements
x
Needle
US focus
FOUS at needle tip
z
Lower variability in lateral direction

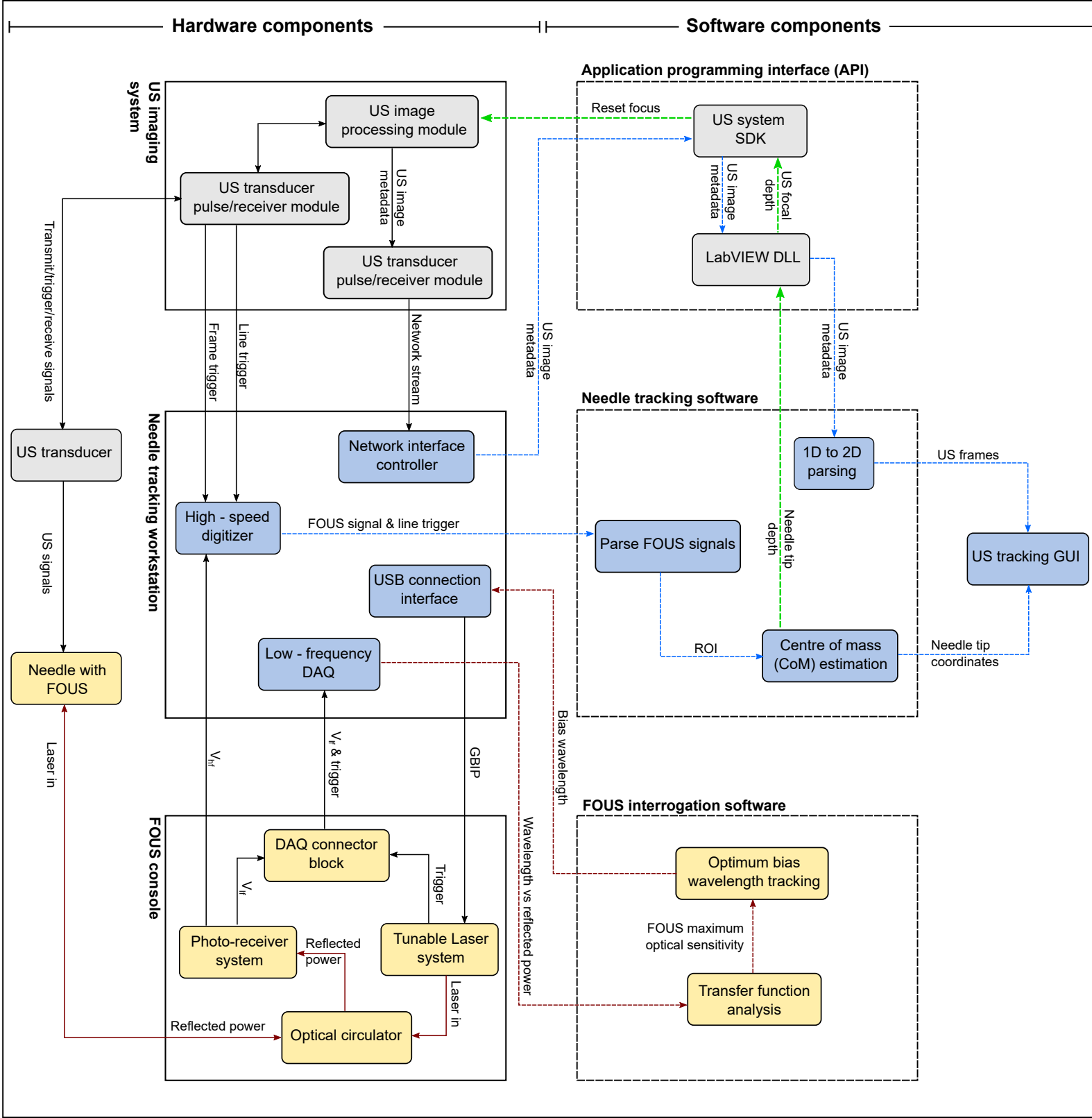
Hardware components
Software components
US imaging system
US image processing module
US transducer pulse/receiver module
US image metadata
US transducer pulse/receiver module
Application programming interface (API)
Reset focus
US system SDK
US image metadata
US focal depth
LabVIEW DLL
Transmit/trigger/receive signals
Frame trigger
Line trigger
Network stream
US image metadata
US image metadata
Needle tracking software
US transducer
Needle tracking workstation
Network interface controller
1D to 2D parsing
US frames
High - speed digitizer
FOUS signal & line trigger
Parse FOUS signals
Needle tip depth
US tracking GUI
US signals
USB connection interface
ROI
Centre of mass (CoM) estimation
Needle tip coordinates
Needle with FOUS
Low - frequency DAQ
Laser in
V_{hf}
V_{lf} & trigger
GBIP
Bias wavelength
FOUS interrogation software
FOUS console
DAQ connector block
Optimum bias wavelength tracking
V_{lf}
Trigger
FOUS maximum optical sensitivity
Photo-receiver system
Reflected power
Tunable Laser system
Wavelength vs reflected power
Laser in
Transfer function analysis
Reflected power
Optical circulator

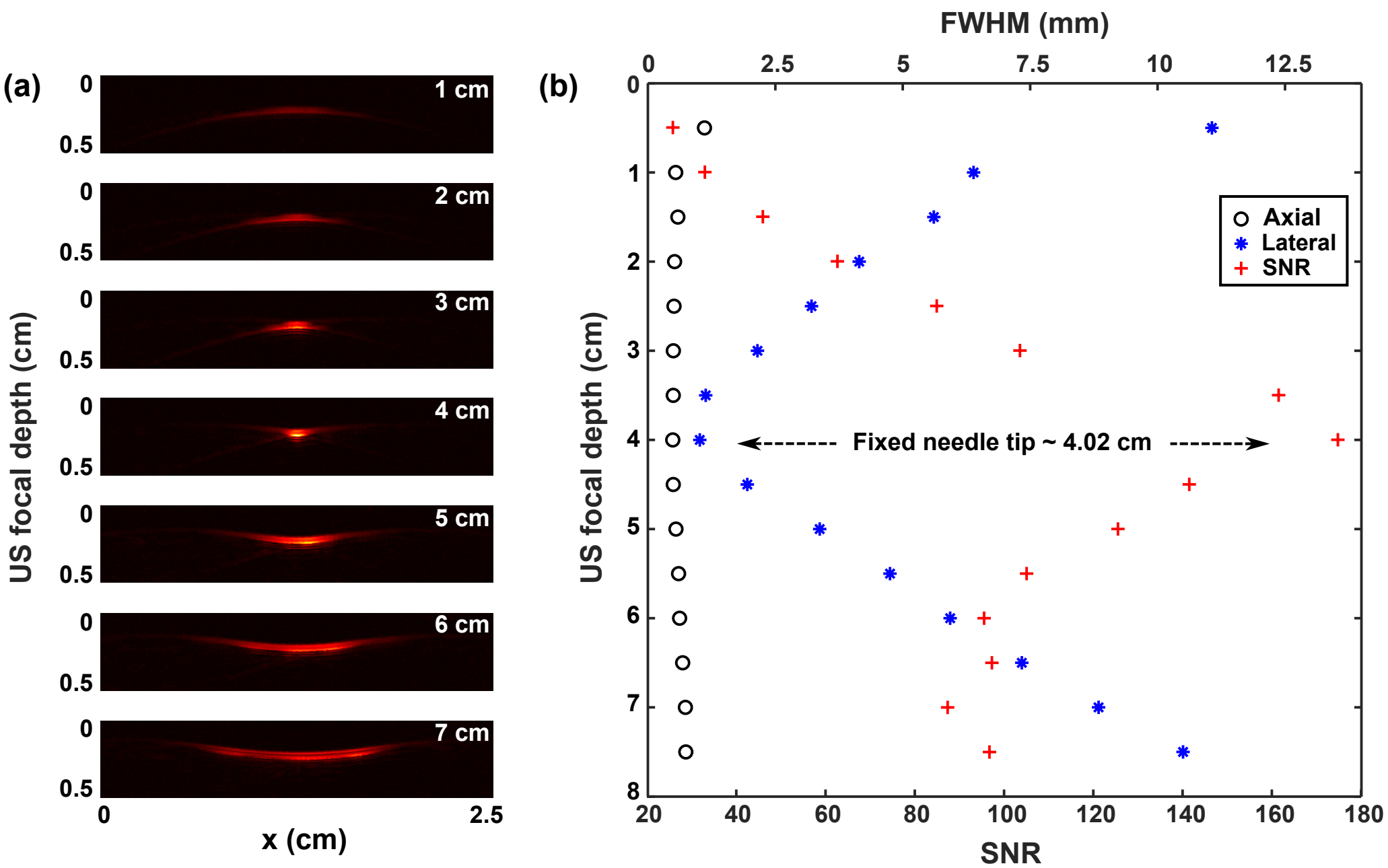
(a)
1 cm
2 cm
3 cm
4 cm
5 cm
6 cm
7 cm
0
0.5
US focal depth (cm)
0
2.5
x (cm)
(b)
FWHM (mm)
0
2.5
5
7.5
10
12.5
Axial
Lateral
SNR
Fixed needle tip ~ 4.02 cm
US focal depth (cm)
0
1
2
3
4
5
6
7
8
20
40
60
80
100
120
140
160
180
SNR

(a) Needle tip images with fixed focus at 4.18 cm

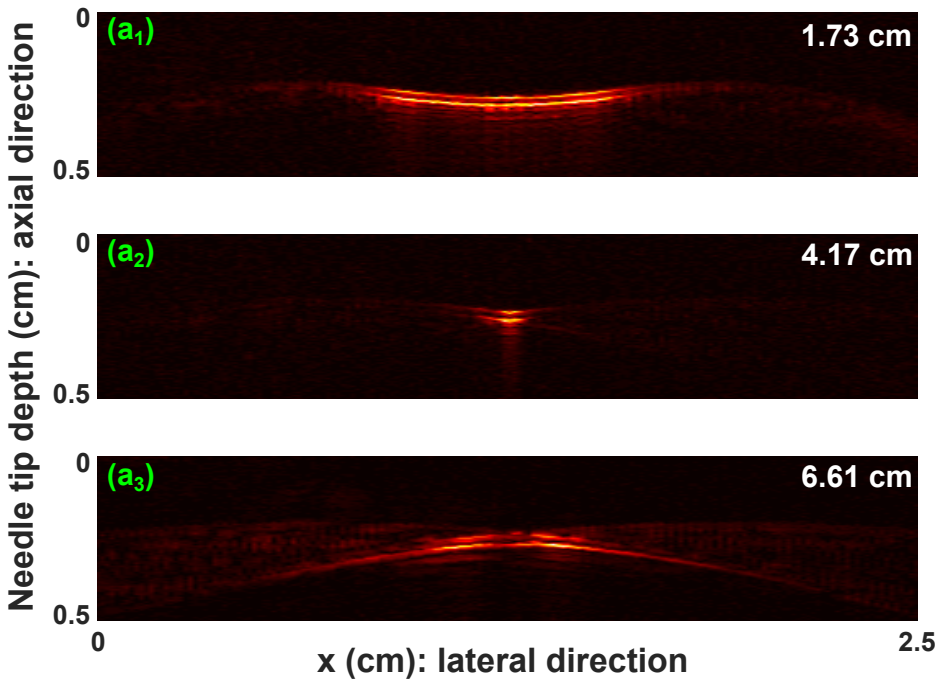

(b) Needle tip images with focus tracking

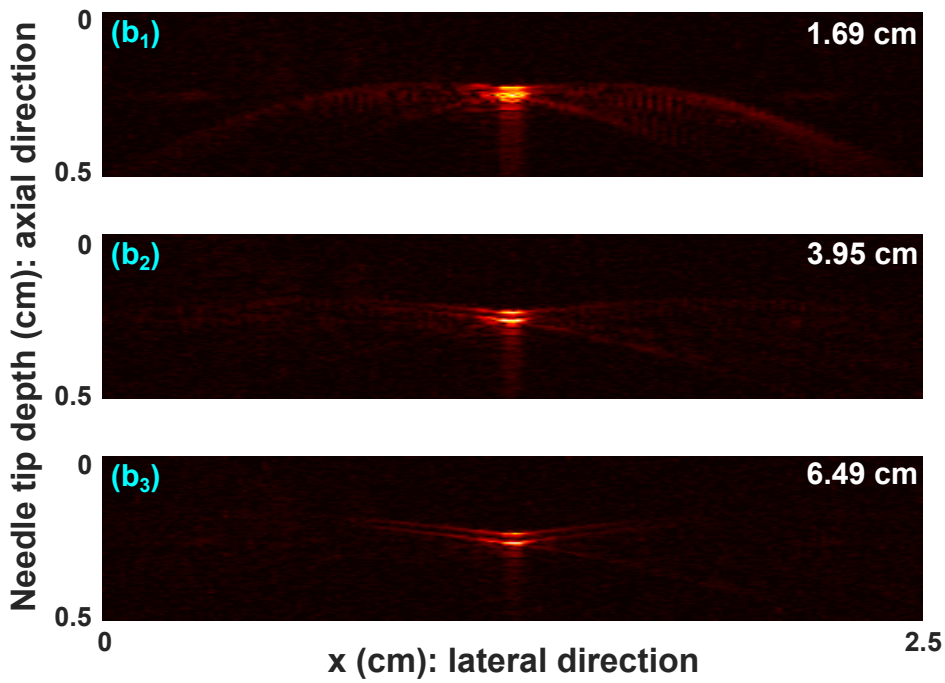

(c) Max variability along lateral direction

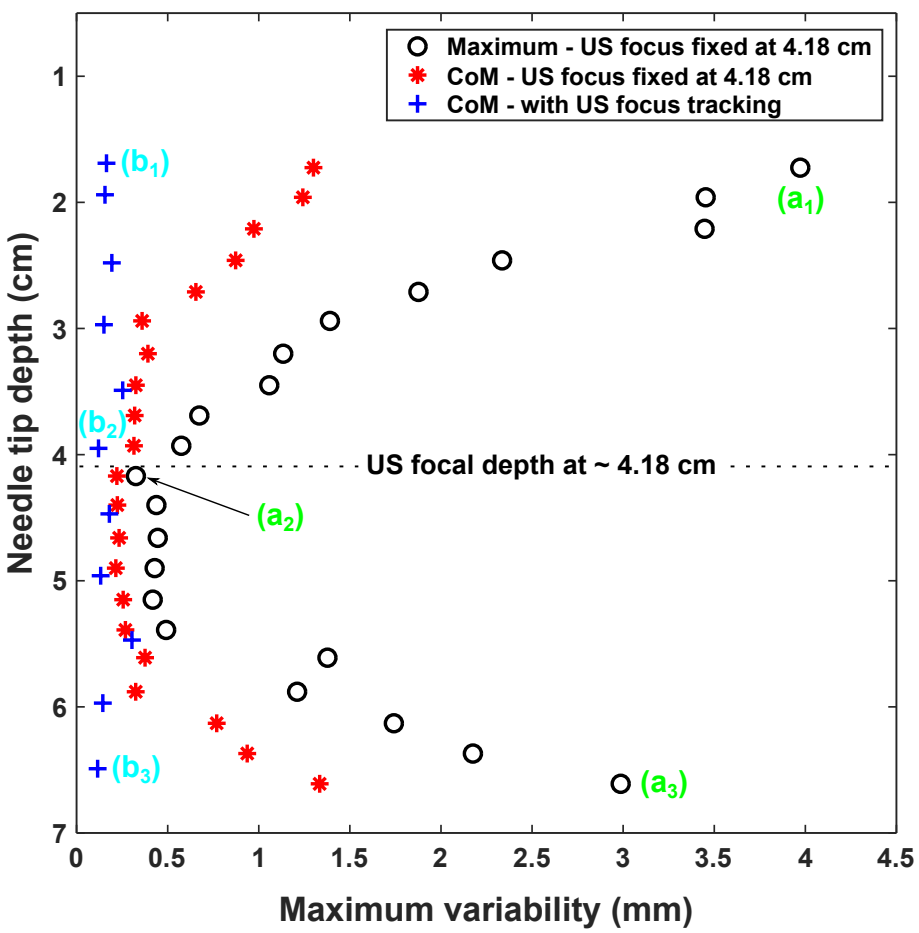

(d) Max variability along axial direction